DOI: 10.1002/ejic.200900560

The Assembly of Phosphometalate Clusters with Copper Complex Subunits

Xiaoming Lu,*[a] Xudong Shi,[a] Yangang Bi,[a] Chong Yu,[a] Yuyou Chen,[a] and Zixiang Chi[a]

Keywords: Polyoxometalates / Organic–inorganic hybrid composites / Solvothermal synthesis / Copper / Molybdenum / Tungsten

Six organic–inorganic hybrid compounds based on a phosphometalate cluster with copper complex subunits: $\{[Cu(phen)_2]_2Cl\}(PMo_{12}O_{40})\cdot H_2O$ (**1**), $\{[Cu(phen)_2]_2Cl\}(PW_{12}O_{40})\cdot H_2O$ (**2**), $[CuI(bpy)_2]_2\{[CuII(bpy)]_2P(Mo^V)_3(Mo^{VI})_9O_{40}\}$ (**3**), $H[Cu(bpy)(H_2O)]\{[Cu(bpy)]_4(PO_4)_2\}(PW_{11}CuO_{39})\cdot H_2O$ (**4**), $[Cu(phen)(H_2O)]_3[(PO_4)_2Mo_5O_{15}]\cdot 5H_2O$ (**5**), and $HNa[Cu(bpy)(H_2O)]_2[(PO_4)_2Mo_5O_{15}]\cdot 6H_2O$ (**6**) (phen = 1,10-phenanthroline, bpy = 2,2′-bipyridine) have been solvothermally synthesized. Single-crystal X-ray diffraction reveals that compounds **1** and **2** are composed of a Keggin polyoxoanion $(PM_{12}O_{40})^{3-}$ (M = Mo, W) and $\{[Cu(phen)_2]_2Cl\}^{3+}$ counterion. Compound **3** is built from two $[Cu^I(bpy)_2]^+$ cations and a reduced-Keggin polyoxoanion $[PMo^V{}_3Mo^{VI}{}_9O_{40}]^{6-}$ which is bi-capped by two $[Cu^{II}(bpy)]^{2+}$ through four bridging oxo groups on two opposite (Mo_4O_4) faces. Compound **4** is based on a monovacant Keggin anion $(PW_{11}CuO_{39})^{5-}$ linked through four $Cu(bpy)^{2+}$, two PO_4^{3-}, and one $\{H[Cu(bpy)(H_2O)]\}^{3+}$, generating a one-dimensional chain. Compounds **5** and **6** exhibit a chain-like structure constructed from $[(PO_4)_2Mo_5O_{15}]^{6-}$ clusters linked through $[Cu(phen)(H_2O)]^{2+}$ and $[Cu(bpy)(H_2O)]^{2+}$ components, respectively. The pH is crucial for the isolation of the compounds. Compounds **1** and **2** are obtained in the pH range 1–2 with the phen ligand, and **3** and **4** are isolated in the pH range 3–4 and 2–3 with the bpy ligand, respectively. Oxalic acid acting as a reductant reduces the molybdenum ion from Mo^{VI} to Mo^V in **3**. Compounds **5** and **6** are produced in the pH range 3–4 with phen and bpy ligands, respectively. Compound **3** shows fluorescence due to the charge transfer from Cu^I-to-ligand (MLCT) [d^{10}-π^*]. Compound **4** displays magnetic behavior based on the super-interaction through the tricopper six-membered ring [Cu^{II}–O–Cu^{II}–O–Cu^{II}–O–].

Introduction

Polyoxometalates (POMs),[1] as early transition-metal oxide clusters, have excited considerable interest in solid-state materials chemistry, because of their structural and compositional diversity, and great potential applications in catalysis, sorption, ion exchange, optical, electro and magnetic materials.[2] Recently, an intriguing area of research in this field has been the construction of inorganic–organic materials based on POMs. Several successful strategies have been developed to design such materials.[3] One of the promising methods is to connect POM building units with secondary transition-metal complexes acting as inorganic bridging groups under hydrothermal or solvothermal conditions. The transition-metal complexes can dramatically influence the inorganic oxide microstructure, so we can combine the merit of POMs and transition-metal complexes to constitute some interesting compounds with unique properties. Many examples have been explored recently, including discrete clusters,[4] one-dimensional chains,[5] two-dimensional networks,[6] and three-dimensional frameworks.[7] Systematic structural design of composite materials possessing unique structures and potentially useful magnetic and luminescent properties remains extremely challenging. However, several successful strategies have been developed to design such materials.[8] One utilizes the polyoxometalates's coordination ability to produce polyoxoanion-supported or bridged by transition metal or lanthanide cations under hydrothermal or solvothermal conditions, providing charge-compensation, space-filling, passivating and structure-directing roles.[9] In particular, Zubieta's and Wang's group have reported a series of such hybrid materials consisting of polyoxomolybdate and phosphomolybdate clusters attached to various transition-metal complexes, such as $[Ni(3,4'\text{-bpy})_2MoO_4]3H_2O$,[6c] $[Cu(terpy)Mo_2O_7]$,[5c] $Na_2[\{Mn(phen)_2(H_2O)\}\{Mn(phen)_2\}_3\{MnMo_{12}O_{24}(HPO_4)_6(PO_4)(OH)_6\}]\cdot 4H_2O$,[6b] $[\{Cu(2,2'\text{-bpy})\}\{Cu(IN)_2\}\{Mo_4O_{12}(OH)_2\}]$,[7d] and $[\{Cu_3(trz)_2\}V_4O_{12}]$[7a] etc. We have extended the approach above by introducing a copper metal cation as an additional structural component in the construction of a coordination complex cation which provides charge-compensation, space-filling, and structure-directing roles. And herein, we report the solvothermal synthesis and crystal structure of six compounds $\{[Cu(phen)_2]_2Cl\}(PMo_{12}O_{40})\cdot H_2O$ (**1**), $\{[Cu(phen)_2]_2Cl\}(PW_{12}O_{40})\cdot H_2O$ (**2**),

[a] Department of Chemistry, Capital Normal University, P. O. Box, 100048 Beijing, China
E-mail address: lu-xiaoming@126.com
Supporting information for this article is available on the WWW under http://dx.doi.org/10.1002/ejic.200900560.

$[Cu^{I}(bpy)_2]_2\{[Cu^{II}(bpy)]_2P(Mo^{V})_3(Mo^{VI})_9O_{40}\}$ (**3**), $H[Cu(bpy)(H_2O)]\{[Cu(bpy)]_4(PO_4)_2\}(PW_{11}CuO_{39})\cdot H_2O$ (**4**), $[Cu(phen)(H_2O)]_3[(PO_4)_2Mo_5O_{15}]\cdot 5H_2O$ (**5**), and $HNa[Cu(bpy)(H_2O)]_2[(PO_4)_2Mo_5O_{15}]\cdot 6H_2O$ (**6**) (phen = 1,10-phenanthroline, bpy = 2,2′-bipyridine). Both compounds **1** and **2** consist of a discrete a Keggin PM_{12} phosphometalate anion and a copper complex counterion through static interaction. Compound **3** is also composed of copper complex cations and a Keggin PMo_{12} phosphometalate cluster, however, three Mo^{VI} are reduced to Mo^{V} and bi-capped by two copper complex subunits oppositely. Compound **4** forms a one-dimensional chain-like structure based on a monovacant PW_{11} phosphometalate cluster linked by a copper complex subunit via coordination bonds. Compounds **5** and **6** also form a chain-like structure however based on a P_2M_5 phosphometalate cluster linked by a copper complex subunit via coordination bonds. The pH is crucial for the formation of the six compounds noted above.

Results and Discussion

Synthesis

The isolation of compounds **1**, **2**, **3**, **4**, **5**, and **6** depended on solvothermal techniques, because differential solubility of organic and inorganic precursors can be minimized. However, factors such as temperature, starting materials, pressure, acidity, reactant, stoichiometry, and time of reaction can influence the reaction. Parallel experiments show that pH is crucial for isolation of compounds **1**–**6**. Compounds **1** and **2** can only be obtained in the pH range 1–2. Compounds **3** and **4** are produced in the pH range 2–3 and 3–4, respectively. Compounds **5** and **6** can be synthesized in the pH range 3–4. At higher pH (pH ≧ 5) no crystal was formed but a mixture of powders, probably due to decomposition of the polyanion at high pH. The effect of the starting materials for the reactions is also important. When $Cu(NO_3)_2\cdot 6H_2O$ was replaced by other compounds containing Cu^{II} such as $CuCl_2\cdot 2H_2O$, $CuSO_4\cdot 5H_2O$, or $CuAc_2\cdot 2H_2O$ in identical hydrothermal reaction environments, compound **4** could not be obtained. The effect of the different starting compounds containing Cu^{II} on the crystallization of the final product is still under study. Oxalic acid is essential for the structural difference between **3** and **4**, as it can reduce molybdenum from Mo^{VI} to Mo^{V}, whereas it could not reduce tungsten from W^{VI} to W^{V}. Compounds **5** and **6** based on $[(PO_4)_2Mo_5O_{15}]^{6-}$ are produced in the pH range 3–4 with the ligands bpy and phen, respectively; however, their tungsten analogs could not be crystallized in the same hydrothermal reaction environment.

Structures

Single-crystal X-ray diffraction analysis was performed on compounds **1**–**6** and showed that the six compounds are all based on phosphometalate clusters with copper complex subunits. The polyhedral representation of compounds **1** and **2** is shown in Figure 1. Compound **2** is the tungsten analog of **1**. Both are composed of one α-Keggin $(PM_{12}O_{40})^{3-}$ (M = Mo, W) anion and a $\{[Cu(phen)_2]_2Cl\}^{3+}$ cation. The valence sum calculations confirm that all M (M = Mo or W) and Cu atoms are +6 and +2, respectively. Similar to the well-known α-Keggin structure, $(PM_{12}O_{40})^{3-}$ consists of a central PO_4 tetrahedron which is in disorder and shares the four O atoms with four M_3O_{13} units. Each M_3O_{13} is constituted by three MO_6 shared faces. In $\{[Cu(phen)_2]_2Cl\}^{3+}$, the Cl^- acts as a bridge linked to two Cu^{II} from two $Cu(phen)^{2+}$ cations, and every Cu^{II} coordinates with four N atoms from two phen ligands in a distorted 4+1 square prism geometry. The bond lengths of Cu–N and Cu–Cl are 1.982(7)–2.095(6) Å and 2.42(2)–2.440(2) Å, respectively. The discrete phosphometalate anions and the copper complex cations co-present in the crystal lattice through static force and π-π stacking interaction for the phen ligand (Figure 2).

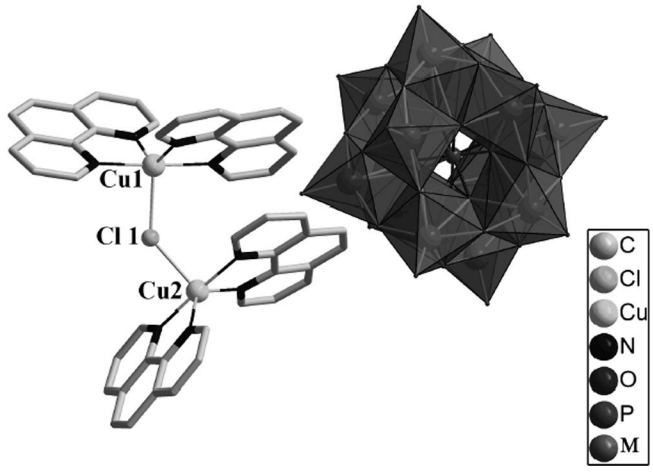

Figure 1. Polyhedral representation of compounds **1** and **2**, of which M = Mo for **1** and W for **2**. Hydrogen atoms and lattice water are omitted for clarity and the PO_4 is in disorder.

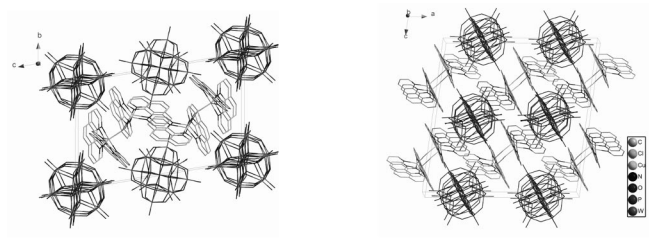

Figure 2. View of the packing diagram of compound **1** along the *a*-axis (a) and **2** along the *b*-axis (b), showing that phen are integrated via π-π stacking interaction.

The structure of compound **3** (Figure 3) consists of a $\{[Cu^{II}(bpy)]_2PMo^{V}_3Mo^{VI}_9O_{40}\}^{2-}$ heteropolyoxoanion and two $[Cu^{I}(bpy)_2]^{+}$ counterions. Valence sum calculations give the average valence of 5.70 for Mo atoms (the expected

average valence for $Mo^{V}_{3}Mo^{VI}_{9}$ is 5.75), showing 3 of 12 Mo atoms in +5 oxidation state with three electrons delocalized within the whole metal-oxide cluster. Valence sum calculations also indicate that Cu(1, 2) and Cu(3, 4) are +2 and +1, respectively. A typical feature of the structure is that the reduced-Keggin polyoxoanion $[P(Mo^{V})_3(Mo^{VI})_9O_{40}]^{6-}$ with more negative charge is bi-capped by two $[Cu^{II}(bpy)]^{2+}$ (Cu1, Cu2) forming a coordinated $\{[Cu^{II}(bpy)]_2PMo^{V}_{3}Mo^{VI}_{9}O_{40}\}^{2-}$ anion through four bridging oxo groups on two opposite $\{Mo_4O_4\}$ faces. The Cu^{II}–O distances are 1.999(4)–2.372(4) Å and Cu^{II}–N distances are 1.987(5)–2.001(5) Å, and the coordination geometry is a $(Cu^{II}O_4N_2)$ octahedron. However, as counter cations Cu^{I} (Cu3, Cu4) ions are only coordinated with four N atoms from two bpy ligands [Cu^{I}–N, 1.992(7)–2.052(8) Å] in a distorted tetrahedron ($Cu^{I}N_4$), and interact with $\{[Cu^{II}(bpy)]_2PMo^{V}_{3}Mo^{VI}_{9}O_{40}\}^{2-}$ by static attraction. Another feature is that the Cu^{II}(1, 2) is six- and Cu^{I}(3, 4) is four-coordinate separately in this structure.

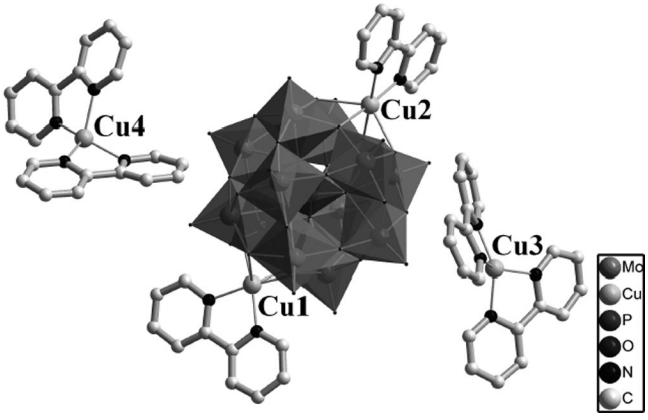

Figure 3. The molecular structure of compound **3**, of which Cu^{II} is Cu(1) and Cu(2), whereas Cu^{I} is Cu(3) and Cu(4). Octahedra, (MoO_6); tetrahedra, (PO_4).

The basic building block of compound **4** is composed of one defective-heteropolyoxoanion $(PW_{11}CuO_{39})^{5-}$, two PO_4^{3-}, and five $Cu(bpy)^{2+}$ ions (Figure 4). The valence sum calculations confirm that all W and Cu atoms are +6 and +2, respectively. The Cu(1) in the heteropolyoxoanion $(PW_{11}CuO_{39})^{5-}$ occupies the vacancy of the defective $(PW_{11}O_{39})^{7-}$ anion and is bound to the POM by five oxygen atoms (Figure 5). The unusual structural feature of **4** is that the monovacant Keggin anion $(PW_{11}CuO_{39})^{5-}$ is linked by five $Cu(bpy)^{2+}$ and two PO_4^{3-}, generating a one-dimensional chain (Figure 6, a). According to their coordination type shown in part b of Figure 6, the PO_4 tetrahedron can be divided into three groups: one (P1) is located in the center of $(PW_{11}O_{39})^{7-}$; the second (P2) has a terminal O(42), two μ_2-O(O41, O43), and one μ_3-O(40) atoms; and the third (P3) possesses two μ_2-O(O45, O47) and two μ_3-O(46, 44) atoms. Cu atoms can be also divided into three groups: Cu(1) is in a (CuO_6) distorted octahedral geometry coordinated by one oxygen from PO_4^{3-} and five oxygen atoms from $(PW_{11}O_{39})^{7-}$ with Cu–O distances of 1.938(11)–2.325(11) Å; Cu(4) is four-coordinate, with two nitrogen atoms from a bpy and two oxygen atoms from two different PO_4 tetrahedra, with Cu–O distances of 1.901(11)–2.018(10) Å and a Cu–N distance of 1.977(14)–1.980(14) Å; Cu(2, 3, 5, 6) are coordinated by two nitrogen atoms from bpy and three oxygen atoms, showing square-pyramidal geometry in the form of (CuN_2O_3), with a Cu–O distance of 1.902(11)–2.356(10) Å and Cu–N distance of 1.954(15)–2.034(14) Å. Meanwhile, Cu(5) is bound to the terminal oxygen atom (O9) of the POM, resulting in the one-dimensional chain.

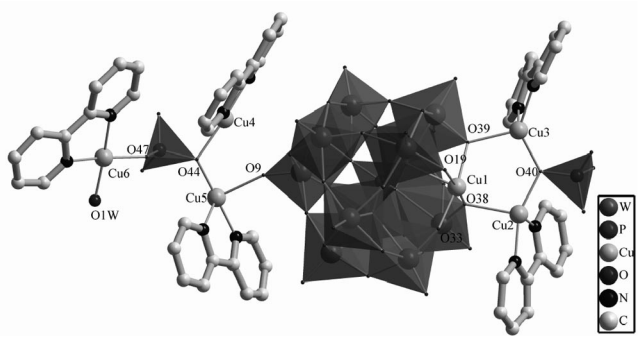

Figure 4. The basic building block of compound **4**, H atoms and lattice water are omitted for clarity. Octahedra, (WO_6); tetrahedra, (PO_4).

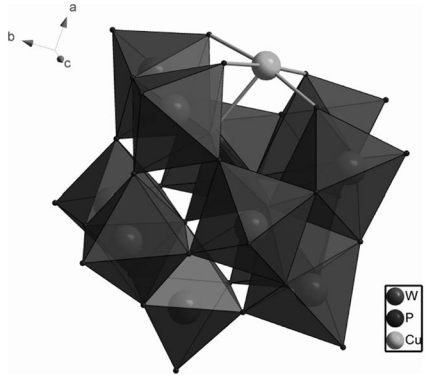

Figure 5. Polyhedral structure of $(PW_{11}Cu^{II}O_{39})^{5-}$.

The basic building block of compound **5** is shown in Figure 7; there are three crystallographically unique Cu atoms in the asymmetric unit, and all of them are coordinated in a distorted (CuN_2O_3) "4+1" square-pyramidal geometry, of which the two N atoms are from one phen ligand, two O atoms are from the (P_2Mo_5) cluster, and one O atom is from the water molecule. The Cu–N and Cu–O distances are in the range of 2.002(4)–2.037(4) Å, and 1.946(3)–2.329(3) Å, respectively. According to the architecture of compound **5**, the copper complex cations may be divided into three types: the complex $[Cu(1)(phen)(H_2O)]^{2+}$ subunit links to only one (P_2Mo_5) cluster through two O atoms, one from a terminal oxygen of the PO_4 tetrahedra, and the other from μ_2-O (Mo–O–Mo); the $[Cu(2)(phen)(H_2O)]^{2+}$ component is bound to two (P_2Mo_5) clusters via two O atoms, one from

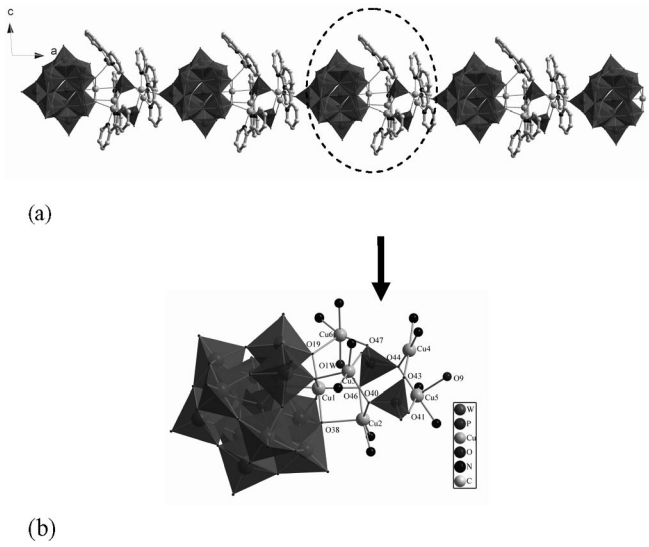

Figure 6. (a) View of the one-dimensional chain assembled by compound **4**; (b) the coordination environments of Cu^{II} and PO_4^{3-} in compound **4**. All C and H atoms are omitted for clarity.

a terminal oxygen of the PO_4 tetrahedra, the other from a terminal oxygen of the MoO_6 octahedra of the adjacent (P_2Mo_5) cluster; the $[Cu(3)(phen)(H_2O)]^{2+}$ complex is similar to the Cu(2) complex, but of the two O atoms one is a terminal oxygen of the MoO_6 octahedra, and the other is from μ_2-O(Mo–O–P) belonging to the adjacent (P_2Mo_5) cluster. So each (P_2Mo_5) cluster is bridged by $[Cu(2,3)(phen)(H_2O)]^{2+}$ subunits to assemble the one-dimensional infinite chain (Figure 8). It is interesting that the one-dimensional chain is like a propeller, with (P_2Mo_5) as the center and the three copper complexes as blades in three directions.

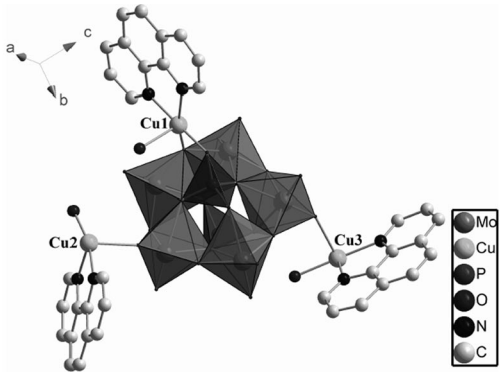

Figure 7. The basic building block of compound **5**. Hydrogen atoms and lattice water are omitted for clarity. Octahedra, (WO_6); tetrahedra, (PO_4).

The structure of compound **6**, shown in Figure 9, is similar to that of **5**. However, there is one crystallographically unique Cu atom in the asymmetric unit, and it also adopts a distorted square-pyramidal geometry (CuN_2O_3) "4+1" coordination mode, of which the two N atoms are from one bpy ligand, one O atom is from a terminal oxygen of the PO_4 tetrahedra of (P_2Mo_5), one O atom is from a terminal

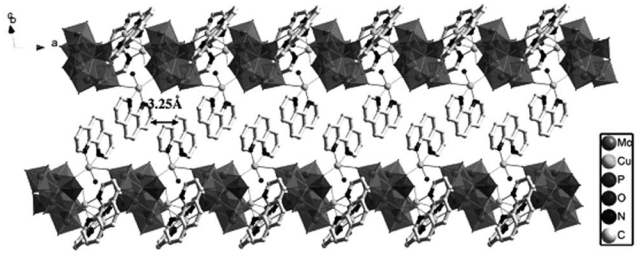

Figure 8. View of the one-dimensional chain of compound **5**, showing the (P_2Mo_5) clusters linked through Copper complexes, and the π–π stacking interaction between the aromatic rings. Hydrogen atoms and lattice water are omitted for clarity. Octahedra, (MoO_6); tetrahedra, (PO_4).

oxygen of the MoO_6 octahedra of the adjacent (P_2Mo_5) cluster, and one O atom is from a water molecule. The most remarkable feature compared with compound **5** is that there is a Na ion exactly deposited between two (P_2Mo_5) clusters, interacting with eight oxo ligands of the polyanion with a Na–O distance ranging from 2.480(3) Å to 2.720(3) Å; the coordination environment of Na is represented in Figure 10. Each (P_2Mo_5) cluster is linked by $[Cu(bpy)(H_2O)]^{2+}$ subunits to assemble the one-dimensional infinite chain (Figure 11). According to the bridging mode of the oxo ligands, the O atoms can be divided into two types, one is O(2,2A), O(11,11A), and O(12,12A) which serve as μ_3-O bridges forming a 12-membered ring with heteroatoms (Cu,

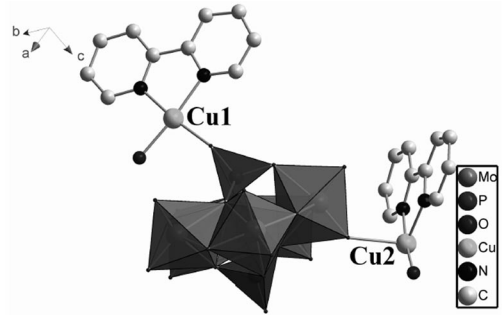

Figure 9. The basic building block of compound **6**. Octahedra, (WO_6); tetrahedra, (PO_4).

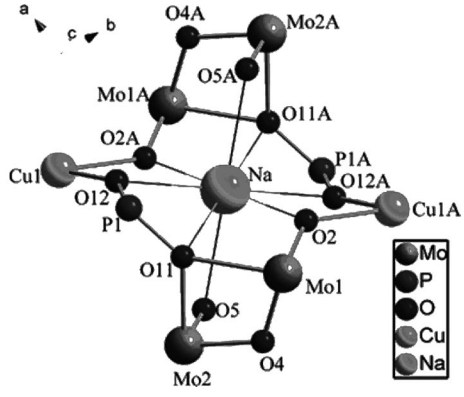

Figure 10. The drawing of coordination environments of Na in compound **6**.

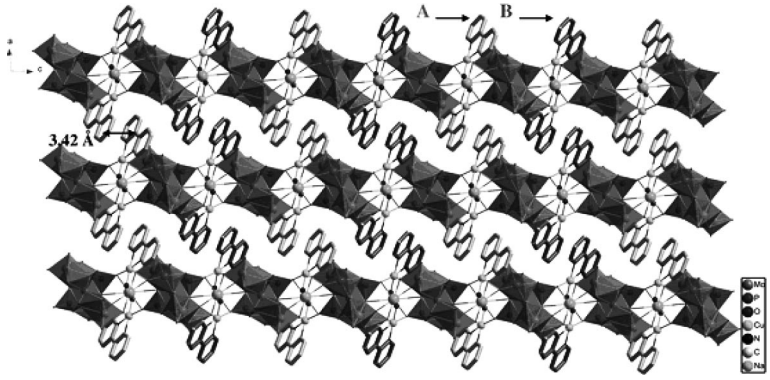

Figure 11. View of the one-dimensional chain of compound **6**, showing two types of aromatic rings.

Mo, and P) containing a Na ion in the center. The other is O(5,5A) which adopts μ_2-O mode (Na–O–Mo), capping each side of the ring. Like compound **5**, in compound **6** there is also a weak interaction between the one-dimensional chains via π-π stacking existing between the adjacent interchain aromatic rings of 2,2′-bipyridine at a face–face distance of 3.42 Å. However, the striking difference between the two compounds is that there are two types (A and B) of aromatic rings in **6**, with the two types of aromatic ring vertical to each other along the chain (Figure 11). Thereby, the π-π stacking interaction only exists in the same ring type. Also hydrogen bonding is observed in **6**, with O–H···O and C–H···O distances ranging from 2.605–2.895 Å and 2.974–3.283 Å, respectively. The structure of **6** manifests two of the noncovalent forces, hydrogen bonding and π–π stacking interactions.

Comparing the structures of the six compounds, it is found that the unsaturated feature of the phosphometalates either in valence or geometry plays an important part in the formation of coordinated organo-phosphometalate derivatives. Compounds **1** and **2**, with the well-known Keggin structure $(PM_{12}O_{40})^{3-}$ [M = Mo^{VI}, W^{VI}] with T_d symmetry, are both stable in valence and geometry, therefore as a discrete cluster combine with $\{[Cu(phen)_2]_2Cl\}^{3+}$ by static interaction without coordinated linkage between the anion and cation. Whereas in compound **3**, the reduced Keggin structure $[P(Mo^{V})_3(Mo^{VI})_9O_{40}]^{6-}$ has too high a negative charge to be presented individually, so coordinates with $\{[Cu^{II}(bpy)]_2P(Mo^{V})_3(Mo^{VI})_9O_{40}\}^{2-}$ forming an organo-derivative with partial balance in negativity. For compound **4**, the monovacant phosphometalate PW_{11} is unsaturated in geometry, so connects with $Cu(bpy)^{2+}$ forming a $H[Cu(bpy)(H_2O)]\{[Cu(bpy)]_4(PO_4)_2\}(PW_{11}CuO_{39})\cdot H_2O$ coordinated building block which assembles the one-dimensional chain further. Moreover, P_2Mo_5 in compound **5** with the geometry of a defective cluster with lower symmetry and stabilities, is more easily attached to by other units, so ligates with copper complex subunits through bridging O atoms, forming organo-derivative $[Cu(phen)(H_2O)]_3[(PO_4)_2Mo_5O_{15}]\cdot 5H_2O$, which assembles the one-dimensional coordinated chain further. Similar to **5**, compound **6** $HNa[Cu(bpy)(H_2O)]_2$ $[(PO_4)_2Mo_5O_{15}]\cdot 6H_2O$ based on P_2Mo_5, uses bpy instead of phen in constructing another type of chain-like organic–inorganic hybrid structure with the introduction of the Na^+ ion. The unsaturated feature of phosphometalates in geometry and valence can be controlled by pH and redox material separately. Compounds **1** and **2** with perfect phosphometalate are obtained in the pH range 1 to 2, **3** with reduced phosphometalate is prepared in pH 3 to 4, **4** with monovacant phosphometalate is produced in pH 2 to 3, and **5** and **6** with defect phosphometalate are derived in the pH range 3 to 4. The pH can be adjusted with diluted HCl, and the reduction of valences of metals can be achieved using a reductant such as oxalic acid $(C_2H_4O_2\cdot 2H_2O)$.

Thermal Analysis for the Six Compounds

To gain knowledge relating to the thermal stabilities of the organo-POM derivatives, thermal analysis of the six compounds was carried out. The thermal gravimetric analysis (TGA) of compounds **1** and **2** shows that both compounds lose weight in one step, starting at 242, 334 and ending at 732, 768 °C with the weight losses of 28.9% and 21.3%, respectively corresponding to the release of lattice water and ligands, and the calculated values are 27.1% and 19.5%. Compound **3** shows two weight-loss steps: the first in the temperature range 331–523 °C corresponding to the release of four bpy molecules coordinated with Cu^{I} though uncoordinated with polyoxophosphometalate, 19.5% (calcd. 20.8%); the second at 542–663 °C in response to the decomposition of the other two bpy ligands linked both with Cu^{II} and $PMo^{V}_3Mo^{VI}_9$, 10.1% (calcd. 10.4%). Compound **4** shows that chemical decomposition starts at 435 and ends at 752 °C with a weight loss of 19.7%, equivalent to loss of organic ligand (calcd. 19.2%). Compounds **5** and **6** show two weight-loss steps. The first in the temperature range 164–286 °C corresponding to the release of lattice water and ligand water molecules, 8.9% (calcd. 8.1%) for **5**, and at 112–285 °C 8.8% (calcd. 9.5%) for **6**; the second at 382–688 °C in response to the decomposition of the ligands, 31.2% (calcd. 30.4%) for **5**, and at 431–644 °C 21.4% (calcd. 20.6%) for **6**. The thermal analysis indicated that ligands coordinated both with polyoxophosphometalate and the copper ion start decomposing at a higher tem-

perature than those ligands coordinated with copper only. Notably for compound **3**, in which the ligands can be divided into two types according to their coordination environment, one coordinated both with copper and phosphometalate, another coordinated with copper only, the bpy ligands uncoordinated with POMs start decomposing at 331 °C and end at 523 °C, whereas the bpy ligands coordinated with POMs lose their weight from 542–663 °C. It is suggested that we can improve the thermal stability of the organic ligands by coordinating the ligand with POMs.

XPS and Photoluminescence for Compound 3

In order to confirm the valence of Cu^{1}, Cu^{II}, Mo^{V}, and Mo^{VI} in compound **3**, the X-ray photoemission spectroscopy (XPS) of compound **3** was studied (Figure 12, a). The XPS spectrum shows the shoulder peaks of $2p_{3/2}$ and $2p_{1/2}$ at 934.3 and 954.1 eV, respectively, suggesting the presence of Cu^{I}. Satellite peaks at 943.2 and 962.2 eV indicate that the compound also contains Cu^{II}. The XPS spectrum of Mo (Figure 12, b) displays four partially overlapped peaks, and the curve fitting gives the positions of these four peaks at 231.2 eV (a), 232.4 eV (b), 234.3 eV (c), and 235.5 eV (d), ascribed to $Mo^{V}3d_{5/2}$, $Mo^{VI}3d_{5/2}$, $Mo^{V}3d_{3/2}$, and $Mo^{VI}3d_{3/2}$, respectively. These results further confirm the valence of copper and molybdenum of compound **3**.

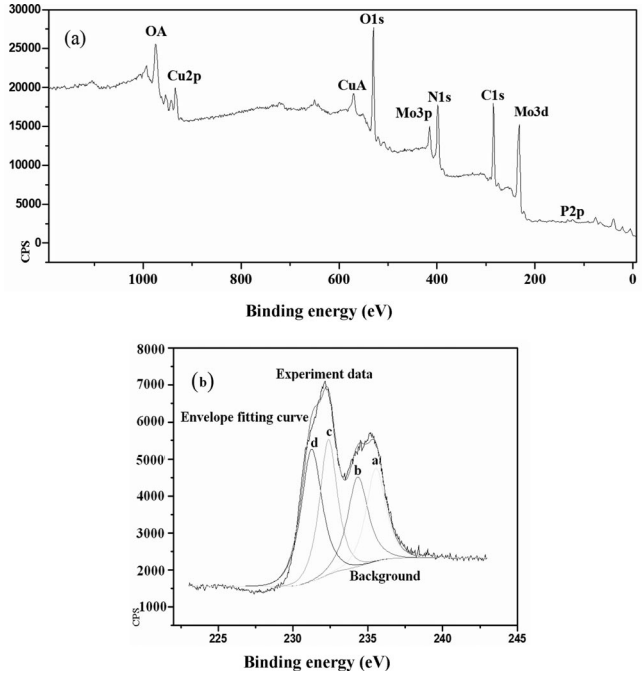

Figure 12. (a) The XPS spectrum of Cu in compound **3**. (b) The XPS spectrum of Mo in compound **3** and its fitting. The peak positions from curve fitting: a 231.2 eV; b 232.4 eV; c 234.3 eV; d 235.5 eV.

Since there is a possibility that the (Cu^{I})-to-ligand charge-transfer can result in fluorescence, the emission spectrum of compound **3** in the solid state at room temperature was determined and is shown in Figure 13. The spectrum exhibits mild blue fluorescent emission bands at ca. 390 nm upon excitation at ca. 246 nm, which are associated with (Cu^{I})-to-ligand charge-transfer (MLCT) [d^{10}-π^*] as we expected. The reduction of copper from Cu^{II} to Cu^{I} which occurred only in compound **3** is the primary origin of the fluorescence, which may be introduced into the preparation of fluorescent POM materials in the future.

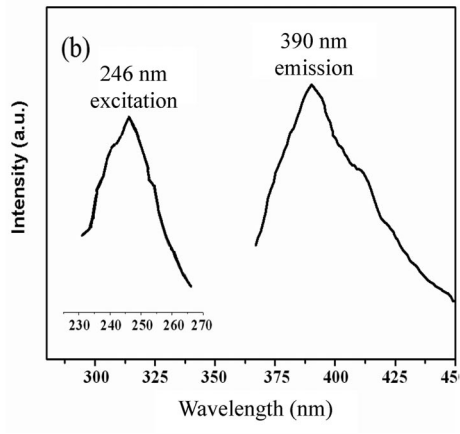

Figure 13. The excitation and emission spectra of compound **3** in the solid state at room temperature.

Magnetic Property of Compound 4

On the basis of the super-interaction through the tri-Cu^{II}-nucleus six-membered ring $Cu^{II}(1)$–O(38)–$Cu^{II}(2)$–O(40)–$Cu^{II}(3)$–O(39)–$Cu^{II}(1)$ in compound **4**, which may potentially possess magnetic features, the magnetic properties of **4** were studied between 2 and 300 K at a field strength of 1000 Oe. The thermal variations of $\chi_M T$ and $1/\chi_M$ are displayed in Figure 14. The $\chi_M T$ curve exhibits a continuous decrease from 3.42 $cm^3 mol^{-1} K$ at 300 K to 1.04 $cm^3 mol^{-1} K$ at 5 K, characteristic of antiferromagnetic interactions among Cu^{II} ions. However, the curve increases a little below 5 K, indicating a very weak ferromagnetic interaction exists in compound **4** at lower temperatures. Above 20 K, the magnetic susceptibility of **4** follows the

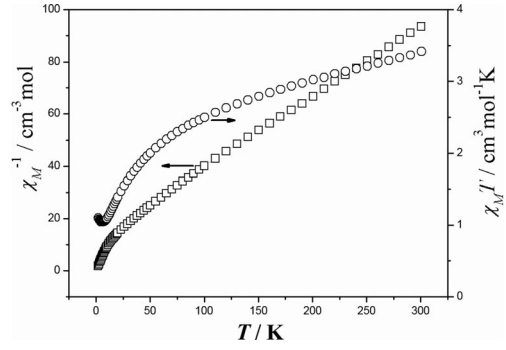

Figure 14. Temperature dependence of $1/\chi_M$ and $\chi_M T$ for compound **4** in an applied field of 1 kOe between 2 and 300 K.

Curie–Weiss law, $\chi_M = C/(T - \theta)$ ($C = 3.60\ cm^3\,mol^{-1}\,K$, $\theta = 39.71$ K), illustrating predominantly antiferromagnetic coupling between Cu^{II} centers. According to the crystal structure of **4**, the magnetic behavior results from super-exchange interactions among the tri-Cu^{II} six-membered ring $Cu^{II}(1)$–O(38)–$Cu^{II}(2)$–O(40)–$Cu^{II}(3)$–O(39)–$Cu^{II}(1)$. In contrast to compound **4**, the other Cu^{II}-related compounds in this paper do not show obvious magnetic properties as there is no Cu^{II}–O–Cu^{II} interaction as in **4**.

Conclusions

We report the synthesis and characterization of six decorated organo-polyoxometalate derivatives, $\{[Cu(phen)_2]_2Cl\}(PMo_{12}O_{40})\cdot H_2O$ (**1**), $\{[Cu(phen)_2]_2Cl\}(PW_{12}O_{40})\cdot H_2O$ (**2**), $[Cu^{I}(bpy)_2]_2\{[Cu^{II}(bpy)]_2P(Mo^{V})_3(Mo^{VI})_9O_{40}\}$ (**3**), $H[Cu(bpy)(H_2O)]\{[Cu(bpy)]_4(PO_4)_2\}(PW_{11}CuO_{39})\cdot H_2O$ (**4**), $[Cu(phen)(H_2O)]_3[(PO_4)_2Mo_5O_{15}]\cdot 5H_2O$ (**5**), and $HNa[Cu(bpy)(H_2O)]_2\ [(PO_4)_2Mo_5O_{15}]\cdot 6H_2O$ (**6**) (phen = 1,10-phenanthroline, bpy = 2,2′-bipyridine) based on phosphometalate clusters with copper complex subunits. The successful isolation of the six compounds indicates that the phosphometalate cluster is a versatile building block that can coordinate with copper complex subunits with different ligands. The polymerization and the structure of the organo-POM derivatives can be modified by adjusting pH and reducing the valence of the metal. The ligands coordinated with both copper and POMs show more stability thermally than those uncoordinated with POMs. The (Cu^{I})-to-ligand charge-transfer (MLCT) [d^{10}-π*] results in fluorescence, which may be used in the preparation of fluorescent organo-POM materials. The super-interaction through Cu^{II}–O–Cu^{II}–O–Cu^{II}–O–Cu^{II} leads to magnetic behavior, opening up a potential new path for magnetic organo-POM hybrid materials.

Experimental Section

General Materials and Methods: All chemicals were purchased from commercial sources and used without further purification. Elemental analyses (C, N, and H) were performed with a Perkin–Elmer 2400 elemental analyzer and P, Cu, W, and Mo were analyzed with a PLASMA-SPEC ICP atomic emission spectrometer. FT-IR spectra were recorded in the range 4000–400 cm^{-1} with an EQUINOX-55 spectrometer using KBr pellets. TGA were performed with a Perkin–Elmer TGA7 instrument in flowing N_2 with a heating rate of 10°min^{-1}. XPS analysis was performed with a VG Scientific ESCALab220i-XL spectrometer with an Al-K_α achromatic X-ray source. Binding energies were referenced to the C1s line at 284.8 eV from adventitious carbon. Excitation and emission spectra were obtained with a RF-5301PC spectrofluorometer equipped with a 450-W xenon lamp as the excitation source, and the measurements were performed at room temperature. Variable-temperature magnetic susceptibility data were obtained with a SQUID magnetometer (Quantum Design, MPMS-7) in the temperature range 2–300 K at 1000 Oe. Samples for the magnetic measurements were ground into powder in order to avoid anisotropy effects.

Synthesis of $\{[Cu(Phen)_2]_2Cl\}(PMo_{12}O_{40})\cdot H_2O$ (1): A mixture of $Na_2MoO_4\cdot 2H_2O$ (0.970 g, 4.01 mmol), $CuCl_2\cdot 2H_2O$ (0.140 g, 0.82 mmol), 2,2′-bipyridine (0.183 g, 1.17 mmol), Phen (0.297 g, 1.65 mmol), H_3PO_4 (85%) (0.438 g), H_2O (15 mL), and CH_3OH (15 mL) was stirred (the initial pH value was adjusted to 1–2 with 2 M HCl) and then sealed in a 30-mL Teflon-lined autoclave, which was heated at 140° for two days. After slow cooling to room temperature, blue block crystals of compound **1** were obtained in 43% yield (based on Cu). $\{[Cu(phen)_2]_2Cl\}(PMo_{12}O_{40})\cdot H_2O$ (2723.61): calcd. C 21.03, H 1.32, N 4.09, Cu 4.64, Mo 41.99; found C 21.43, H 1.75, N 4.39, Cu 4.34, Mo 42.08. Selected FT-IR data (KBr): $\tilde{\nu}$ = 508 (m), 720 (s), 806 (s), 960 (s), 1064 (m), 1428 (m), 1520 (m), 3404 (br) cm^{-1}.

$\{[Cu(Phen)_2]_2Cl\}(PW_{12}O_{40})\cdot H_2O$ (2): Compound **2** was prepared by a procedure similar to that for **1**, but with $Na_2WO_4\cdot 2H_2O$ instead $Na_2MoO_4\cdot 2H_2O$. Yield: 72% (based on Cu). $\{[Cu(phen)_2]_2Cl\}(PW_{12}O_{40})\cdot H_2O$ (3778.53): calcd. C 15.26, H 0.91, N 2.97, Cu 3.36, W 58.39; found C 15.78, H 1.21, N 2.47, Cu 3.45, W 58.43. Selected FT-IR data (KBr): $\tilde{\nu}$ = 518 (m), 722 (s), 814 (s), 894 (s), 976 (m), 1078 (m), 1423 (m), 1522 (m), 3478 (br) cm^{-1}.

$[Cu^{I}(Bpy)_2]_2\{[Cu^{II}(bpy)]_2PMo^{V}_3Mo^{VI}_9O_{40}\}$ (3): A mixture of $Na_2MoO_4\cdot 2H_2O$ (1.115 g, 4.61 mmol), $CuCl_2\cdot 2H_2O$ (0.323 g, 1.89 mmol), 2,2′-bipyridine (0.183 g, 1.17 mmol), oxalic acid ($C_2H_4O_2\cdot 2H_2O$) (0.138 g, 1.44 mmol), H_3PO_4 (85%) (0.470 g), H_2O (15 mL), and CH_3OH (15 mL) was stirred (the initial pH value was adjusted to 3–4 with 2 M HCl) and then sealed in a 50-mL Teflon-lined autoclave, which was heated at 140 °C for two days. After slow cooling to room temperature, black block crystals of **3** were obtained in 40% yield (based on Cu). $[Cu^{I}(bpy)_2]_2\{[Cu^{II}(bpy)]_2PMo^{V}_3Mo^{VI}_9O_{40}\}$ (3013.53): calcd. C 23.91, H 1.61, N 5.58, Cu 8.43, Mo 38.20, P 1.03; found C 23.32, H 2.01, N 5.97, Cu 8.56, Mo 38.02, P 1.25. Selected FT-IR data (KBr): $\tilde{\nu}$ = 491 (m), 763 (m), 945 (s), 1029 (m), 1057 (m), 1174 (m), 1311 (m), 1439 (m), 1597 (m), 3448 (w) cm^{-1}.

$H[Cu(Bpy)(H_2O)]\{[Cu(bpy)]_4(PO_4)_2\}(PW_{11}CuO_{39})\cdot H_2O$ (4): Compound **4** was prepared by a procedure similar to that for compound **3**, but with $Na_2WO_4\cdot 2H_2O$ (1.24 g, 3.76 mmol), 2,2′-bipyridine (0.233 g, 1.49 mmol), and $Cu(NO_3)_26\cdot H_2O$ (0.360 g, 1.22 mmol) (the initial pH value was adjusted to 2–3 with 85% H_3PO_4). Yield: 60% (based on Cu). $H[Cu(bpy)(H_2O)]\{[Cu(bpy)]_4(PO_4)_2\}(PW_{11}CuO_{39})\cdot H_2O$ (4066.49): calcd. C 14.77, H 1.12, N 3.44, Cu 9.38, P 2.29, W 49.73; found C 14.21, H 1.32, N 3.03, Cu 8.99, P 2.87, W 49.03. Selected FT-IR data (KBr): $\tilde{\nu}$ = 520 (m), 814 (s), 882 (m), 957 (s), 1061 (m), 1094 (m), 1448 (m), 1474 (m), 1604 (m), 3448 (br) cm^{-1}.

$[Cu(Phen)(H_2O)]_3[(PO_4)_2\ Mo_5O_{15}]_5\cdot H_2O$ (5): A mixture of $Na_2MoO_4\cdot 2H_2O$ (0.935 g, 3.86 mmol), $CuCl_2\cdot 2H_2O$ (0.312 g, 1.82 mmol), 1,10-phenanthroline (0.297 g, 1.65 mmol), H_3PO_4 (85%) (0.420 g), H_2O (15 mL), and CH_3OH (15 mL) was stirred (the initial pH value was adjusted to 3–4 with 2 M HCl) and then sealed in a 50-mL Teflon-lined autoclave, which was heated at 140 °C for two days. After slow cooling to room temperature blue block crystals of compound **5** were obtained in 40% yield (based on Cu). $[Cu(phen)(H_2O)]_3[(PO_4)_2Mo_5O_{15}]_5\cdot H_2O$ (1786.93): calcd. C 24.22, H 2.26, N 4.71, Cu 10.68, Mo 26.87, P 3.47; found C 24.66, H 2.68, N 4.12, Cu 10.73, Mo 27.01, P 3.78. Selected FT-IR data (KBr): $\tilde{\nu}$ = 567 (m), 721 (s), 917 (s), 1036 (m), 1102 (m), 1148 (m), 1426 (m), 1518 (m), 1628 (w), 3461 (br) cm^{-1}.

$HNa[Cu(bpy)(H_2O)]_2[(PO_4)_2Mo_5O_{15}]\cdot 6H_2O$ (6): Compound **6** was prepared by a procedure similar to that for compound **5**, using 2,2′-bipyridine instead of 1,10-phenanthroline. Yield: 60% (based on Cu). $HNa[Cu(bpy)(H_2O)]_2[(PO_4)_2Mo_5O_{15}]\cdot 6H_2O$ (1517.22): calcd. C 15.83, H 2.19, N 3.69, Cu 8.34, Mo 31.62, Na 1.22, P 4.08; found C 15.21, H 2.68, N 4.031, Cu 8.01, Mo 31.41, Na 0.98,

P 3.88. Selected FT-IR data (KBr): $\tilde{\nu}$ = 582 (m), 694 (s), 917 (s), 1009 (m), 1055 (m), 1110 (m), 1444 (m), 1603 (m), 3454 (br) cm^{-1}.

X-ray Crystallography: Intensity data collection was carried out with a Bruker Smart APEXII diffractometer equipped with a CCD detector using Mo-K_α monochromated radiation (λ = 0.71073 Å) at room temperature. All data were corrected for absorption using SADABS.[10] The structure was solved by direct methods and refined by full-matrix least-squares on F^2 using the SHELXTL-97 software package.[11] All non-hydrogen atoms in compounds **1**–**6** were refined anisotropically. Positions of hydrogen atoms attached to carbon were fixed at their ideal positions. A summary of the crystallographic data and structure determinations for compounds **1**–**6** is provided in Table 1 and Table 2, and the selected lengths and angles are presented in Table 3. The ORTEP drawings of compounds **1**–**6** are given as Supporting Information.

CCDC-737935 (for **1**), -737936 (for **2**), -631873 (for **3**), -633134 (for **4**), -624601 (for **5**), and -631800 (for **6**) contain the supplementary crystallographic date for this paper. These data can be obtained free of charge from The Cambridge Crystallographic Data Centre via www.ccdc.cam.ac.uk/data_request/cif.

Table 1. Crystal data and structure refinement of compounds **1**, **2**, and **3**.

	1	**2**	**3**
Empirical formula	$C_{48}H_{36}ClCu_2N_8O_{42}PMo_{12}$	$C_{48}H_{36}ClCu_2N_8O_{42}PW_{12}$	$C_{60}H_{48}Cu_4N_{12}O_{40}PMo_{12}$
Formula weight	2723.61	3778.53	3013.53
Crystal size [mm^3]	0.42 × 0.33 × 0.19	0.42 × 0.33 × 0.34	0.42 × 0.38 × 0.12
Crystal system	triclinic	monoclinic	monoclinic
Space group	$P\bar{1}$	$C2/c$	$P2_1/c$
Unit cell dimension [Å]			
a	12.6192(3)	24.3267(7)	13.2629(7)
b	13.4093(3)	11.8453(3)	29.7181(15)
c	21.1602(5)	24.4819(6)	21.4910(10)
α [°]	99.4840(10)	90	90
β [°]	94.5890(10)	97.705(2)	103.021(2)
γ [°]	94.8100(10)	90	90
Volume [$Å^3$], Z	3503.16(14), 2	6990.9(3), 4	8252.8(7), 4
$D_{calcd.}$ [$g\,cm^{-3}$]	2.582	3.590	2.425
μ [mm^{-1}], F (000)	2.827, 2600	20.410, 6736	2.878, 5788
Reflections collected	38943	32186	85278
Unique reflections	17265	8657	20286
R_{int}	0.0403	0.0438	0.0596
Final R indices $[I > 2\sigma(I)]$[a]	R_1 = 0.0574, wR_2 = 0.1194	R_1 = 0.0472, wR_2 = 0.0914	R_1 = 0.0542 wR_2 = 0.1089
R indices [all data]	R_1 = 0.0918, wR_2 = 0.1295	R_1 = 0.0665, wR_2 = 0.0964	R_1 = 0.0968 wR_2 = 0.1310
Goodness-of-fit on F^2	1.039	1.073	1.033

[a] $R_1 = \Sigma||F_o| - |F_c||/\Sigma|F_o|$; $wR_2 = \{\Sigma[w(F_o^2 - F_c^2)^2]/\Sigma[w(F_o^2)]\}^{1/2}$.

Table 2. Crystal data and structure refinement of compounds **4**, **5**, and **6**.

	4	**5**	**6**
Empirical formula	$C_{50}H_{45}Cu_6N_{10}O_{49}P_3W_{11}$	$C_{36}H_{40}Cu_3N_6O_{31}P_2Mo_5$	$C_{20}H_{33}Cu_2N_4NaO_{31}P_2Mo_5$
Formula weight	4066.49	1786.93	1517.22
Crystal size [mm^3]	0.42 × 0.36 × 0.24	0.48 × 0.36 × 0.18	0.42 × 0.38 × 0.36
Crystal system	monoclinic	monoclinic	monoclinic
Space group	$P2_1/n$	$P2_1/c$	$C2/c$
Unit cell dimension [Å]			
a	15.7837(5)	8.5491(3)	20.5011(5)
b	24.1950(7)	29.7815(12)	12.5304(3)
c	21.4063(7)	20.6511(8)	16.3835(3)
β	95.252(2)	101.369(2)	95.4030(10)
Volume [$Å^3$], Z	8140.5(4), 4	5154.7(3), 4	4190.01(16), 4
$D_{calcd.}$ [$g\,cm^{-3}$]	3.315	2.283	2.384
μ [mm^{-1}], F (000)	17.164, 7344	2.554, 3440.0	2.673, 2900.0
Reflections collected	84037	52726	18187
Unique reflections	20310	12821	5186
R_{int}	0.1013	0.0474	0.0214
Final R indices $[I > 2\sigma(I)]$[a]	R_1 = 0.0569 wR_2 = 0.1323	R_1 = 0.0403, wR_2 = 0.0919	R_1 = 0.0390, wR_2 = 0.1085
R indices [all data]	R_1 = 0.1164	R_1 = 0.0557,	R_1 = 0.0423,
Goodness-of-fit on F^2	wR_2 = 0.1530 1.032	wR_2 = 0.1013 1.000	wR_2 = 0.1104 1.176

[a] $R_1 = \Sigma||F_o| - |F_c||/\Sigma|F_o|$; $wR_2 = \{\Sigma[w(F_o^2 - F_c^2)^2]/\Sigma[w(F_o^2)]\}^{1/2}$.

Table 3. Selected bond lengths [Å] and angles [°] of compounds **1**–**6**.

Compound **1**[a]			
Cl(1)–Cu(1)	2.426(2)	Cu(1)–Cl(1)–Cu(2)	129.0(1)
Cl(1)–Cu(2)	2.440(2)	N(1)–Cu(1)–N(4)	178.2(3)
Cu(1)–N(1)	1.982(7)	N(4)–Cu(1)–N(2)	97.9(3)
Cu(1)–N(4)	1.991(7)	N(1)–Cu(1)–Cl(1)	89.3(2)
Cu(2)–N(8)	1.988(6)	N(4)–Cu(1)–Cl(1)	92.4(2)
Cu(2)–N(5)	1.994(7)	N(5)–Cu(2)–Cl(1)	91.9(2)
Mo(1)–O(21)#1	1.827(9)	O(8)–Mo(1)–O(21)#1	104.1(4)
Mo(1)–O(13)#1	1.831(8)	O(21)#1-Mo(1)–O(13)#1	96.6(5)
Mo(3)–O(22)	2.008(7)	O(21)#1-Mo(1)–O(16)	157.0(5)
Mo(3)–O(6)#1	2.36(1)	O(13)#1-Mo(1)–O(5)	63.1(3)
Mo(7)–O(27)	2.419(9)	O(12)–Mo(5)–O(46)#1	102.4(4)
Mo(7)–O(25)#2	2.507(9)	P(2)–O(25)–Mo(9)#2	129.7(5)
O(7)–Mo(3)#1	1.801(8)	P(2)–O(26)–Mo(11)#2	125.4(5)
P(2)–O(25)#2	1.457(9)	Mo(11)#2-O(27)–Mo(10)	112.0(3)
O(33)–Mo(12)#2	1.981(8)	Mo(7)–O(27)–Mo(10)	111.2(3)
Compound **2**[b]			
Cl(1)–Cu(1)#1	2.393(2)	Cu(1)#1-Cl(1)–Cu(1)	136.0(2)
Cu(1)–N(4)	1.970(9)	N(1)–Cu(1)–N(3)	95.3(4)
Cu(1)–N(3)	2.073(9)	N(4)–Cu(1)–Cl(1)	88.6(3)
O(2)–P(1)	1.63(1)	C(12)–N(1)–Cu(1)	114.0(7)
O(2)–W(4)	2.46(1)	P(1)–O(2)–O(5)	49.4(5)
O(3)–W(2)#2	2.38(1)	P(1)–O(2)–W(1)	125.8(8)
O(7)–W(4)#2	1.92(1)	W(1)–O(2)–W(6)	96.0(4)
O(14)–W(3)#2	1.909(9)	O(5)–O(2)–W(4)	133.6(8)
P(1)–O(3)#2	1.534(12)	O(5)#2-O(3)–W(2)#2	75.6(7)
W(6)–O(20)#2	1.92(1)	O(3)#2-O(5)–W(2)	66.8(6)
O(15)–W(6)	1.880(10)	O(5)#2-P(1)–O(3)#2	139.2(7)
O(17)–W(4)	1.896(12)	O(5)#2-P(1)–O(4)#2	115.6(7)
O(19)–W(3)	1.874(9)	O(11)–W(1)–O(12)	65.8(7)
O(20)–W(6)#2	1.917(10)	O(17)–W(4)–O(15)	100.9(6)
Compound **3**			
Cu(1)–O(17)	1.999(4)	O(37)–Mo(8)–O(22)	81.17(17)
Cu(1)–N(2)	1.999(5)	Mo(1)–O(18)–Mo(2)	122.72(19)
Cu(1)–O(18)	2.372(4)	Mo(4)–O(27)–Cu(2)	96.76(17)
Mo(8)–O(22)	1.999(4)	Cu(1)–O(17)–Mo(9)	106.85(18)
Mo(1)–O(18)	1.955(4)	Mo(9)–O(37)–Cu(1)	97.11(17)
Cu(2)–O(32)	2.035(4)	Mo(11)–O(32)–Mo(6)	143.9(2)
Cu(2)–O(40)	2.366(4)	Mo(1)–O(18)–Cu(1)	95.98(17)
Cu(2)–N(3)	1.987(5)	Mo(8)–O(3)–Mo(7)	88.15(13)
Mo(11)–O(40)	1.971(4)	P(1)–O(4)–Mo(12)	126.9(2)
Mo(4)–O(27)	1.963(4)	O(4)–P(1)–O(3)	109.2(2)
Cu(3)–N(5)	2.005(7)	O(27)–Cu(2)–O(40)	126.98(13)
Cu(4)–N(9)	2.037(7)	N(4)–Cu(2)–O(27)	111.85(18)
Compound **4**[c]			
Cu(1)–O(39)	1.983(11)	W(2)–O(39)–Cu(1)	118.5(6)
Cu(2)–O(38)	2.311(10)	W(5)–O(9)–Cu(5)	159.0(7)
Cu(3)–O(45)#1	1.906(10)	Cu(1)–O(39)–Cu(3)	114.5(5)
Cu(4)–O(43)#2	1.901(11)	P(1)–O(1)–Cu(1)	120.4(6)
Cu(5)–O(44)	1.985(10)	Cu(1)–O(1)–W(1)	87.1(4)
Cu(6)–O(19)#2	2.356(10)	P(3)–O(44)–Cu(5)	125.5(6)
W(5)–O(9)	1.733(12)	Cu(5)–O(44)–Cu(4)	115.1(5)
W(2)–O(39)	1.809(11)	P(2)–O(40)–Cu(2)	109.5(6)
P(2)–O(40)	1.531(12)	P(3)–O(46)–Cu(2)#2	130.2(7)
P(3)–O(44)	1.574(12)	P(2)–O(43)–Cu(4)#1	128.7(7)
Compound **5**[d]			
Cu(3)–O(21)	1.953(3)	Mo(3)–O(12)	2.017(3)
Mo(1)–O(1)	1.727(3)	O(21)–Cu(3)–O(26)	93.57(13)
Cu(3)–N(5)	2.010(4)	O(21)–Cu(3)–N(6)	94.43(14)
Cu(3)–O(8)#1	2.314(3)	O(19)–Cu(2)–N(4)	93.98(14)
O(8)–Cu(3)#2	2.313(3)	O(19)–Cu(2)–O(1)#2	103.52(13)
Cu(2)–N(3)	2.037(4)	N(4)–Cu(2)–O(1)#2	96.14(14)
Mo(2)–O(12)	1.960(3)	Mo(4)–O(8)–Cu(3)#	147.53(18)
N(2)–Cu(1)	2.008(4)	Mo(1)–O(1)–Cu(2)#1	154.6(2)
O(23)–Cu(1)	1.946(3)	Mo(2)–O(12)–Cu(1)	119.00(14)
O(12)–Cu(1)	2.003(3)	Cu(1)–O(12)–Mo(3)	117.49(15)
O(1)–Cu(2)#1	2.222(3)	P(2)–O(21)–Cu(3)	136.10(18)
Cu(2)–O(1)#2	2.222(3)	Cu(3)–O(21)–Mo(5)	102.87(13)
Cu(2)–O(25)	1.960(3)	P(1)–O(19)–Cu(2)	158.4(2)
P(1)–O(19)	1.502(3)	N(1)–Cu(1)–O(24)	95.16(15)
P(2)–O(21)	1.533(3)	P(2)–O(23)–Cu(1)	117.66(18)
Compound **6**[e]			
Na(1)–O(2)#1	2.636(3)	Cu(1)–O(1 W)	1.960(4)
Na(1)–O(5)#1	2.671(4)	Cu(1)–N(2)	1.996(4)
Na(1)–O(11)#4	2.720(3)	Cu(1)–O(2)#3	2.249(3)
O(12)–Na(1)	2.480(3)	O(12)–Cu(1)–O(2)#3	86.81(14)
Mo(1)–O(2)	1.739(3)	O(12)#4–Na(1)–O(2)#1	68.56(10)
Mo(2)–O(5)	1.724(4)	O(12)#4–Na(1)–O(5)#1	91.61(11)
Mo(2)–O(11)#1	2.200(3)	O(5)#3–Na(1)–O(11)#4	63.66(10)
P(1)–O(11)	1.556(3)	Mo(1)#1-O(11)–Na(1)	96.06(11)
P(1)–O(12)	1.519(3)	Mo(2)#1-O(11)–Na(1)	94.44(11)
O(12)–Cu(1)	1.936(3)	P(1)–O(11)–Na(1)	87.88(13)

[a] Symmetry transformations used to generate equivalent atoms: #1 $-x + 2, -y + 2, -z + 2$; #2 $-x + 1, -y, -z + 1$; #3 $-x, -y, -z + 1$;. [b] #1 $-x + 2, y, -z + 1/2$; #2 $-x + 3/2, -y + 3/2, -z$. [c] #1 $x + 1, y, z$; #2 $x - 1, y, z$. [d] #1 $x + 1, y, z$; #2 $x - 1, y, z$. [e] #1 $-x, y, -z + 1/2$; #3 $x, -y + 1, z + 1/2$; #4 $-x, -y + 1, -z + 1$.

Supporting Information (see also the footnote on the first page of this article): ORTEP drawings and IR spectra of compounds **1**–**6**.

Acknowledgments

The authors are thankful for the financial support from National Natural Science Foundation of China (No. 20871085) and Beijing Natural Science Foundation (No. 2092009).

[1] M. T. Pope, *Heteropoly and Isopoly Oxometalates*, Springer, Berlin, **1983**.

[2] a) "Introduction: Polyoxometalates Multicomponent Molecular Vehicles To Probe Fundamental Issues and Practical Problems" (Guest Ed.: C. L. Hill), *Chem. Rev.* **1998**, *98*, 1–2 (special issue on polyoxometalates), and references cited therein; b) M. T. Pope, A. Müller, *Angew. Chem. Int. Ed. Engl.* **1991**, *30*, 34–48.

[3] a) P. J. Hagrman, D. Hagrman, J. Zubieta, *Angew. Chem. Int. Ed.* **1999**, *38*, 2638–2684; b) D. Hagrman, P. Hagrman, J. Zubieta, *Inorg. Chim. Acta* **2000**, *300–302*, 212–224; c) R. S. Rarig, R. Lam, P. Y. Zavalij, J. K. Ngala, R. L. LaDuca, J. E. Greedan, J. Zubieta, *Inorg. Chem.* **2002**, *41*, 2124–2133; d) L. Lisnard, A. Delbecq, P. Mialane, J. Marrot, E. Codjovi, F. Se'cheresse, *Dalton Trans.* **2005**, 3913–3920; e) Z. Han, H. Ma, J. Peng, Y. Chen, E. Wang, N. Hu, *Inorg. Chem. Commun.* **2004**, *7*, 182–185.

[4] a) L. Chen, Y. Wang, C. Hu, L. Feng, E. Wang, N. Hu, H. Jia, *J. Solid State Chem.* **2001**, *161*, 173–176; b) M. Yuan, Y. Li, E. Wang, C. Tian, L. Wang, C. Hu, *Inorg. Chem.* **2003**, *42*, 3670–3676.

[5] a) E. Burkholder, V. Golub, C. J. O'Connor, J. Zubieta, *Inorg. Chem. Commun.* **2004**, *7*, 363–366; b) Y. Lu, Y. Xu, E. Wang, J. Lu, C. Hu, L. Xu, *Cryst. Gowth Des.* **2005**, *5*, 257–260; c) E. Burkholder, N. G. Armatas, V. Golub, C. J. O'Connor, J. Zubieta, *J. Solid State Chem.* **2005**, *178*, 3145–3151.

[6] a) Y. Li, G. De, M. Yuan, E. Wang, R. Huang, C. Hu, N. Hu, H. Jia, *Dalton Trans.* **2003**, 331–334; b) M. Yuan, E. Wang, Y. Lu, Y. Li, C. Hu, N. Hu, H. Jia, *J. Solid State Chem.* **2003**,

170, 192–197; c) R. L. LaDuca, M. Desiak, R. S. Rarig, J. Zubieta, *Inorg. Chim. Acta* **2002**, *332*, 79–86.
[7] a) P. J. Hagrman, C. Bridges, J. E. Greedan, J. Zubieta, *J. Chem. Soc., Dalton Trans.* **1999**, 2901–2903; b) D. G. Allis, R. S. Raig, E. Burkholder, J. Zubieta, *J. Mol. Struct.* **2004**, *688*, 11–31; c) R. L. LaDuca, C. Brodkin, R. C. Finn, J. Zubieta, *Inorg. Chem. Commun.* **2000**, *3*, 248–250; d) J. Lu, E. Shen, M. Yuan, Y. Li, E. Wang, C. Hu, L. Xu, J. Peng, *Inorg. Chem.* **2003**, *42*, 6956–6958.
[8] a) P. J. Hagrman, D. Hagrman, J. Zubieta, *Angew. Chem. Int. Ed.* **1999**, *38*, 2638–2684; b) D. Hagrman, P. Hagrman, J. Zubieta, *Inorg. Chim. Acta* **2000**, *300–302*, 212–224; c) R. S. Rarig, R. Lam, P. Y. Zavalij, J. K. Ngala, R. L. LaDuca, J. E. Greedan, J. Zubieta, *Inorg. Chem.* **2002**, *41*, 2124–2133; d) Z. Han, H. Ma, J. Peng, Y. Chen, E. Wang, N. Hu, *Inorg. Chem. Commun.* **2004**, *7*, 182–185.
[9] a) H. An, Y. Li, D. Xiao, E. Wang, C. Sun, *Cryst. Growth Des.* **2006**, *6*, 1107–1112; b) J. Wang, J. Zhao, X. Duan, J. Niu, *Cryst. Growth Des.* **2006**, *6*, 507–513; c) A. Bagno, M. Bonchio, A. Sartorel, G. Scorrano, *Eur. J. Inorg. Chem.* **2000**, 17–20; d) R. S. Rarig, J. Zubieta, *Polyhedron* **2003**, *22*, 177–188.
[10] G. M. Sheldrick, *SADABS, Program for Empirical Absorption Correction of Area Detector Data*, University of Göttingen, **1996**.
[11] G. M. Sheldrick, *SHELX-97, Program for Crystal Structure Refinement*, University of Göttingen, Germany, **1997**.

Received: June 20, 2009
Published Online: November 6, 2009

